This paper appears as K. Dinesh, M. Xiong, J. Adams, R. Dorsey, and G. Sharma, "Signal analysis for detecting motor symptoms in parkinson's and huntington's disease using multiple body-affixed sensors: A pilot study," in Proc. IEEE Western NY Image and Signal Proc. Workshop (WNYISPW) , Nov. 2016.

SIGNAL ANALYSIS FOR DETECTING MOTOR SYMPTOMS IN PARKINSON'S AND HUNTINGTON'S DISEASE USING MULTIPLE BODY-AFFIXED SENSORS: A PILOT STUDY

Karthik Dinesh[⋆], *Mulin Xiong*[†], *Jamie Adams*[†], *Ray Dorsey*[†], *Gaurav Sharma*[⋆]

[⋆] Department of Electrical and Computer Engineering, University of Rochester,Rochester NY
[†] Center for Human Experimental Therapeutics, University of Rochester Medical Center, Rochester NY

ABSTRACT

We report on a pilot study for signal processing based detection and analysis of motor symptoms associated with Parkinson's and Huntington's diseases. In contrast with prior studies using prototype body-worn sensors, that are typically obtrusive, we use light-weight, low-power sensors that can be affixed to the body like adhesive temporary tattoos, allowing for unobtrusive attachment of multiple sensors for continuous motion measurement over durations of up to 48 hours. Signal analysis of the accelerometer data from the sensors highlights the benefit of the proposed approaches: clear signatures are seen for different clinically observed motor symptoms either in the signals recorded in a specific sensor, or in the inter-relations across sensor signals.

***Index Terms*—** Wearable sensors, Parkinson's, Huntington's, accelerometer, health analytics

1. INTRODUCTION

Sensor technologies are currently undergoing development at a rapid pace making available low-power, small-footprint, low-cost sensors for measuring a number of physical quantities. Signal processing algorithms that leverage the large amounts of data collected by such sensors are enabling many new applications. In this paper, we report on a pilot study that focuses on the analysis of data from multiple light-weight body-affixed sensors to analyze motor symptoms associated with motion irregularities in Parkinson's disease (PD) [1] and Huntington's disease (HD) [2].

PD and HD are chronic neurological conditions that cause movement disorders in affected individuals. PD is characterized by involuntary tremors of the limbs, stiffness and slowness in movement accompanied by episodes of gait freezing up and postural instability. HD is an inherited disease characterized by erratic jerky movements in the body, referred to as *chorea*, and uncoordinated movement of the limbs that results in an unsteady gait. Additionally, cognitive impairment is also commonly observed in HD. No cures are currently available for PD/HD. Although, medications are used to control symptoms their efficacy is neither universal nor complete and quality of life is often severely degraded for PD/HD patients. It is estimated that within the United States over a million individuals are living with PD [3] and about 30,000 with HD [4]. Despite the relatively smaller numbers, the greater debilitation caused by HD, makes it also of very significant clinical concern.

Motor symptoms, either rhythmic or erratic, are inherent in both PD and HD and these are primarily assessed via in-clinic observations through the Unified Parkinsons Disease Rating Scale (UPDRS) [5] and the Unified Huntingtons Disease Rating Scale (UHDRS) [6], respectively. While these tools are invaluable in clinical practice, they are limited by the short observation time available in the clinic and by the subjective nature of manual assessment. The use of wearable sensors and automated signal analysis is therefore an attractive option for obtaining longer duration data and objective quantitative metrics for tracking disease progression, medication efficacy, for categorizing subjects for personalized medicine, and for early prognosis [7].

While several prior studies have used wearable sensors for analysis of motion disorders in PD/HD [8, 9, 10, 11], these prior sensors have typically been quite obtrusive, which not only causes significant discomfort to the subjects but also potentially influences subjects' body movements, impacting the resulting analysis. In this paper, we report on a pilot study conducted with a newly introduced commercial sensor [12] that is light-weight and unobtrusive and can be applied to the body, much like an adhesive bandage or a temporary tattoo, allowing for ready attachment of multiple sensors to different body parts of the subjects. Specifically, in this pilot study, we focus on accelerometer data for analysis of motion and highlight how the use of multiple sensors significantly simplifies and enhances the signal analysis: clear signatures of individual clinically identified motor symptoms of interest in PD/HD can be seen either by analyzing data from specific sensors or by using the data in coordination across the sensors.

This paper is organized as follows. In Section 2 we describe the key specifications of the sensor and give a brief overview about the clinical study set-up. In Section 3 we describe the analysis performed on the data obtained from multiple body affixed accelerometer sensors to detect signatures for the motor symptoms in PD and HD subjects. We conclude the paper with a discussion and conclusion in section 4.

2. SENSOR AND CLINICAL STUDY SET-UP

The study used MC10 Inc.'s BioStampRC sensors, which are shown in Fig. 1. The sensors is a light weight (≈ 7 gms), multi-mode adhesive sensor capable of operating in different modes, varied sampling rates and dynamic range with high power and long duration capabilities. The key specifications of the sensor are shown in Table 1 [12].

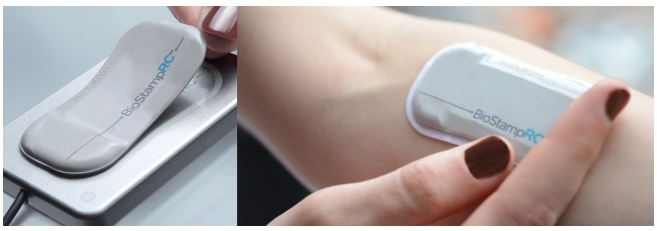

Fig. 1: BioStampRC affixable sensor from MC10 Inc.

This work was supported in part by a gift from MC10 Inc. to the University of Rochester.

This paper appears as K. Dinesh, M. Xiong, J. Adams, R. Dorsey, and G. Sharma, "Signal analysis for detecting motor symptoms in parkinson's and huntington's disease using multiple body-affixed sensors: A pilot study," in Proc. IEEE Western NY Image and Signal Proc. Workshop (WNYISPW) , Nov. 2016.

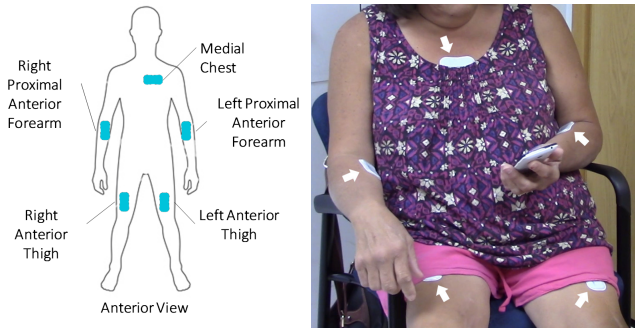

(a) (b)

Fig. 2: (a) Graphics showing the body locations for applying sensors in our study. (b) Participant wearing the sensors at five locations shown in (a) for in-clinic assessment.

For our study, we utilize the accelerometer mode with a sampling rate of 31.25 Hz.

Mode	Sampling Rate	Dynamic Range	Recording Time (Max)
Accelerometer (Accel.)	31.25, 50, 100, 200 Hz	2, 4, or 8 G	8-35 hours
ECG	125, 250 Hz	0.2 V	17-35 hours
EMG	250 Hz	0.2 V	17 hours
Accel.+ECG	50 Hz(accel) 125, 250 Hz (ECG)	2, 4, or 8 G (accel) 0.2 V (ECG)	11-22 hours
Accel.+EMG	50 Hz(accel) 250 Hz(EMG)	2, 4, or 8 G (accel) 0.2 V (EMG)	11 hours
Gyro.+Accel	25, 50, 100, 250 Hz	2, 4, 8, 16 G (accel) Off, 250, 500, 1000, 2000 /sec (gyro)	2-4 hours

Table 1: Key specifications of the BioStampRC sensor from MC10 Inc.

A clinical study was conducted where 16 PD (mean age=68.3 years), 10 HD (mean age=55.9 years) and 15 control (mean age=63.8 years) participants were enrolled and were asked to wear five accelerometer based BioStampRC sensors on chest and limbs as shown in Fig. 2 for the standardized in-clinic assessments and two days at home. A participant survey was conducted to get a feedback on their experience with the sensors. The survey revealed that about 85-90% of participants were comfortable, with the sensors not interfering in their daily activities. Participants were pleased with overall experience and showed willingness to reuse if required.

3. SIGNAL ANALYSIS FOR DETECTING PD AND HD MOTOR SYMPTOMS

In this section we present results from selected analyses of the data obtained from the sensors to detect the motor symptoms in PD/HD. Specifically, we focus on analysis of gait to identify characteristics that differentiate HD from controls and analysis of at rest tremors in PD subjects to highlight the effect of medication on PD subjects.

A. Gait analysis for HD: For the analysis of gait, three 10 meter walk tests were conducted in clinical settings for 10 HD subjects and 15 controls with the sensors on their body. If we observe the gait of the HD subjects, a lack of co-ordination between the legs can be observed when compared to the controls. Due to lack of co-ordination,

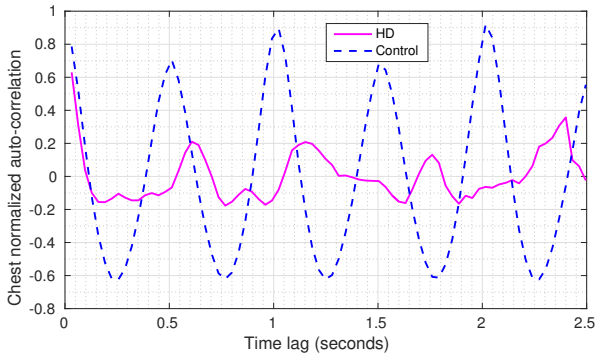

(a)

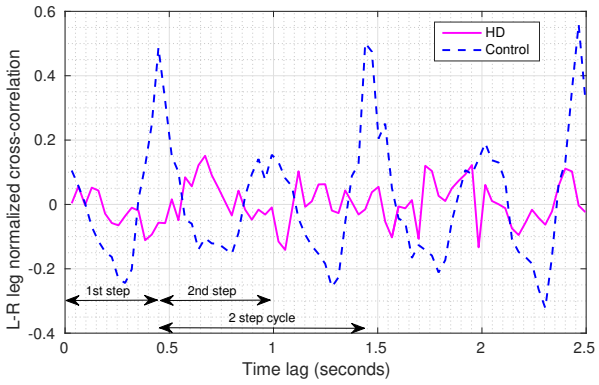

(b)

Fig. 3: (a)Normalized vector auto-correlation of the data from chest sensor as a function of time lags for HD and control. (b) Normalized vector cross-correlation of the data from left leg and right leg sensors as a function of time lags for HD and control with an annotation indicating a 2-step cycle.

we can also observe variation in the step duration of the HD subjects in comparison with controls. In order to characterize the step duration and the lack of co-ordination between the legs, we look at both, single and joint utilization of the sensors. To parameterize the lack of co-ordination between legs, we use normalized vector cross correlation of the data obtained from the sensors attached to the left and right leg. To mitigate the effect of gravity, the cross-correlation analysis is performed after mean subtraction. For a 10 meter walk test instantiation, $\mathbf{a}_L(n)$ and $\mathbf{a}_R(n)$ for $n = 1, 2..., N$ represent the $N \times 3$ mean subtracted data from sensor in the left leg and right leg, respectively, with each row representing three dimensional sample from the tri-axial accelerometer and N representing total number of samples. The normalized vector cross-correlation $R_{LR}(m)$ as a function of time lag m between $\mathbf{a}_L(n)$ and $\mathbf{a}_R(n)$ is then given by,

$$R_{LR}(m) = \frac{\sum_{n=1}^{N-m} (\mathbf{a}_L(n)\mathbf{a}_R(n+m))}{\left(\sum_{n=1}^{N-m} \|\mathbf{a}_L(n)\|^2\right)^{1/2} \left(\sum_{n=1}^{N-m} \|\mathbf{a}_R(n+m)\|^2\right)^{1/2}}. \quad (1)$$

Plots of normalized vector cross-correlation for one 10 meter walk test are shown in the Fig. 3b, for one individual with HD and for one control. Typically, a peak with high magnitude occurs in the cross-correlation at the time when the left foot matches the right foot which happens for control at around 0.5 second and 1.5 second lag, whereas

This paper appears as K. Dinesh, M. Xiong, J. Adams, R. Dorsey, and G. Sharma, "Signal analysis for detecting motor symptoms in parkinson's and huntington's disease using multiple body-affixed sensors: A pilot study," in Proc. IEEE Western NY Image and Signal Proc. Workshop (WNYISPW) , Nov. 2016.

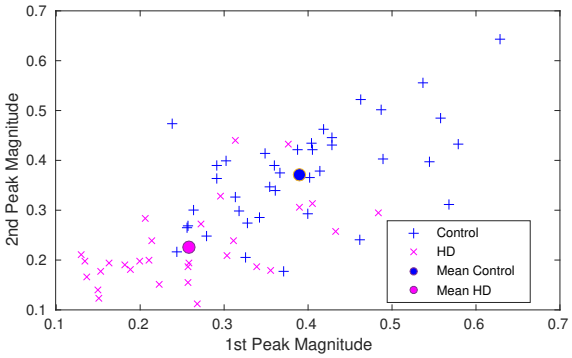

Fig. 4: Scatter plot showing the 1st peak and 2nd peak magnitude of the left-leg to right-leg acceleration vector cross-correlations for all 10 meter walk tests for the individuals with HD and for the control cohort.

for the HD we do not see clear peaks which is an indication for lack of co-ordination between the legs. Using the the 1st peak and the 2nd peak magnitude as features we obtain the scatter plot shown in Fig. 4. The plot shows two distinct clusters corresponding to the HD and control individuals. While the clusters overlap, statistically, a good separation can be seen between the HD and controls with mean magnitude of 1st and 2nd peak being 0.258 and 0.225 for HD and 0.39 and 0.372 for the controls. Apart from the peak magnitudes, another distinguishing feature is the average step duration. From Fig. 3b we can observe that 2 step cycle for control takes about 1 second which indicates a step duration of about 0.5 seconds. For the HD individuals, however, estimating step duration using cross-correlation is challenging.

To analyze the step duration, we utilize the chest sensor which captures movement from both legs and compute the normalized vector auto-correlation of the mean subtracted data. For a 10 meter walk test instantiation, $\mathbf{a}_C(n)$ for $n = 1, 2, ..., N$ represent $N \times 3$ mean subtracted data from sensor in the chest, with each row representing three dimensional sample from the tri-axial accelerometer and N representing total number of samples. The normalized vector auto-correlation for $\mathbf{a}_C(n)$ is given by,

$$R_{CC}(m) = \frac{\sum_{n=1}^{N-m} (\mathbf{a}_C(n)\mathbf{a}_C(n+m))}{\left(\sum_{n=1}^{N-m} \|\mathbf{a}_C(n)\|^2\right)^{1/2} \left(\sum_{n=1}^{N-m} \|\mathbf{a}_C(n+m)\|^2\right)^{1/2}}, \quad (2)$$

where $R_{CC}(m)$ represents the normalized auto-correlation of the chest sensor at the time lags m. Fig. 3a includes plots of normalized vector auto-correlation for same walk tests for the HD and control that were previously used for the cross-correlation analysis. Here we can clearly observe the step cycles and obtain the step duration as the difference between successive peaks in the auto-correlation. The figure shows a consistent step duration with mean step duration of about 0.5 seconds for the control whereas for the HD individual, we observe that there is variation in the step duration with mean step duration of 0.63 seconds. This variation can be attributed to lack of co-ordination and varied velocity and cadence while walking that HD subjects exhibit. The analyses is summarized in the box plot in Fig. 5. We can observe higher variability in step duration with the median value of 0.544 seconds for HD subjects whereas there is limited variability in controls with median value of 0.512 seconds.

B. Analysis of at rest tremors in PD: The aim here is to characterize the effects of medication on the motor symptoms for the PD

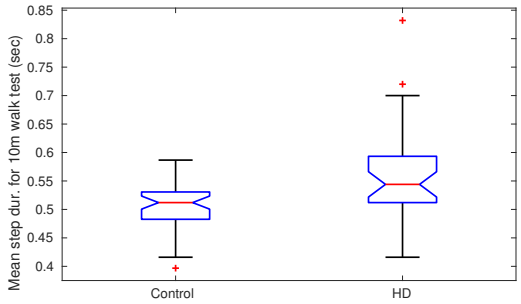

Fig. 5: Comparison of variability in step duration for HD and control based on the normalized vector auto-correlation of chest sensor accelerometer recordings.

subjects with severe and mild tremors. Motor symptoms in PD can been seen in the form of at rest tremors which have rhythmic nature and a typical frequency [13]. For the analysis of at rest tremors, in-clinic postural tremor and rest tremor tests were conducted over a duration of 50 seconds each for 16 PD subjects with the sensors affixed to their body. For 11 out of 16 PD subjects, the tests were conducted in on/off medication phases. Based on the in-clinic UPDRS motor

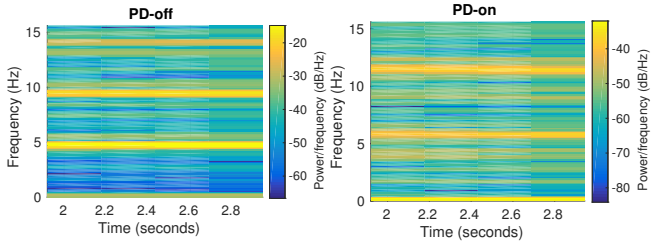

Fig. 6: Spectrogram showing energy distribution as a function of frequency for a PD participant with severe tremor: (a) off medication and (b) on medication. Strong energy peaks can be seen at the typical tremor frequency and its harmonics. On medication the relative energy in these peaks is reduced.

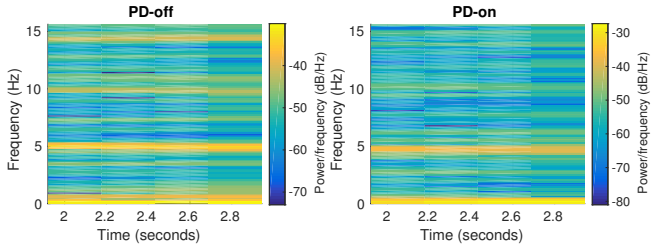

Fig. 7: Spectrogram showing typical tremor frequency and its harmonics for a participant with mild tremor: (a) off medication and (b) on medication.

assessment score, PD subjects were divided in mild tremor and severe tremor categories. Since the at rest tremors are more prevalent in hands, we look at data from the sensors attached to left and right hand. For an instantiation of the rest/postural tremor test, $\mathbf{a}_S(n)$ for $n = 1, 2, ..., N$ represent the $N \times 3$ data (approximately N=1550 samples) from right/left hand sensor. We perform a moving average

This paper appears as K. Dinesh, M. Xiong, J. Adams, R. Dorsey, and G. Sharma, "Signal analysis for detecting motor symptoms in parkinson's and huntington's disease using multiple body-affixed sensors: A pilot study," in Proc. IEEE Western NY Image and Signal Proc. Workshop (WNYISPW) , Nov. 2016.

mean subtraction to counter the effect of gravity on the data to obtain $\mathbf{a}_S^{ma}(n)$ which is also a $N \times 3$ matrix. Apart from moving average mean subtraction we can also utilize the method of calibrating the accelerometers using the quiescent gravity [14] to negate the effect. Instead of analyzing the tri-axial data, we perform principal component analysis (PCA) [15] on $\mathbf{a}_S^{ma}(n)$ and choose the first principal component given by $a_S^{pc}(n)$ which is now a vector of length N. The data $a_S^{pc}(n)$ is divided into segments of 5 second duration (segment sample size=156) using a non-sliding window and we visualize each of these segments using the spectrogram [16] analysis. Given the focus on at rest tremors that have a characteristic frequency, parameters of the spectrogram are chosen to optimize frequency resolution. If $a_{Sl}^{pc}(n)$ represents the l^{th} segment, the short time Fourier transform (STFT) is given by,

$$A_{Sl}(k,\omega) = \sum_{n=-\infty}^{\infty} a_{Sl}^{pc}(n) w(n-k) e^{-j\omega n}, \tag{3}$$

where $w(n)$ represents the window function of length M and k represents the amount of overlap. Discretizing the continuous frequency space, we obtain,

$$A_{Sl}(k,p) = A_{Sl}(k,\omega) \ , at \ \omega = \frac{2\pi}{M} p, \tag{4}$$

The squared magnitude of the discretized STFT gives the spectrogram

$$S(k,p) = |A_{Sl}(k,p)|^2 . \tag{5}$$

The window function $w(n)$ is chosen as a Hamming window and length is chosen to be 128 samples (for each segment sample size of 156) to get a high frequency resolution. Fig. 6a and 6b shows

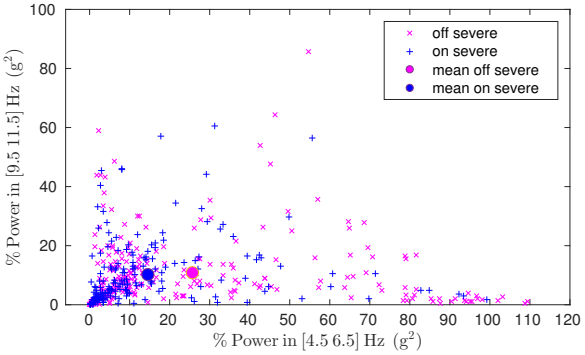

Fig. 8: Scatter plot of relative power in the fundamental and first harmonic bands of the characteristic tremor frequency for on/off medication assessments for PD participants with severe tremors.

the spectrogram of one of the segment from the data of a participant having severe tremor for off and on medications respectively whereas Fig. 7a and 7b shows the spectrogram of participant having mild tremor for off and on medications respectively. In the spectrogram we can clearly see that the tremor has a fundamental frequency around 5Hz and its harmonics. Power in the fundamental frequency and the harmonics for on medication is lower when compared to off medication indicating the impact of medication on PD subjects with severe tremor. It means that although the rate at which the hand shakes remains the similar in off/on cases, the intensity of the shake is reduced on medication. Similarly, in case of mild tremor, we can observe a concentration of power in the typical tremor frequency and harmonics with reduced strength for the on medication scenario

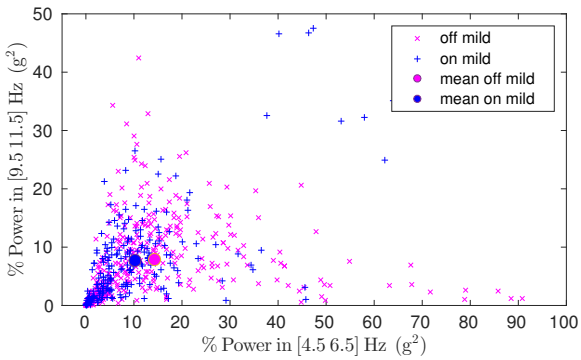

Fig. 9: Scatter plot of relative power in the fundamental and first harmonic bands of the characteristic tremor frequency for on/off medication assessments for PD participants with mild tremors.

though with smaller change than for the severe tremor individual. We use, percentage power (fraction of total power) in fundamental frequency band of [4.5 6.5]Hz and percentage power in the first harmonic band of [9.5 11.5]Hz as two features, obtaining the scatter plots shown in Fig. 8 and Fig. 9, for severe tremor and mild tremor respectively. The scatter plots shown in Fig. 8 for severe tremor reveal that on medication, the mean power in the [4.5 6.5]Hz and [9.5 11.5]Hz bands reduces from 25.61 % and 10.9% to 14.45% and 10.35%. This significant reduction in power indicates a corresponding reduction in the severity of the tremor. Similarly, in Fig. 9, on medication, the mean power in [4.5 6.5]Hz and [9.5 11.5]Hz bands reduces from 14.2 % and 7.9% to 10.23% and 7.71%. Even in mild tremor cases, the severity of the tremors is lower on medication, though the effect is less-pronounced than the severe tremor cases.

4. CONCLUSION AND DISCUSSION

The data and analysis presented in this paper highlight that signal analysis of light-weight body-affixed sensors can detect motor symptoms associated with PD and HD. While the results presented here considered only limited analysis and were based on a relatively small population of study participants, they serve to highlight the utility of multiple sensors. The identification of particular clinically identified motor symptoms is simplified by using either targeted analysis of data from a specific sensor or by investigating the inter-relation of the data across different sensors. Specifically, in our case, the analysis of: (a) step duration for HD was most effectively conducted from the chest sensor data where the variation across steps was minimal, (b) limb coordination in HD was facilitated by considering the cross-correlation between the left and right leg sensors, and (c) at rest tremors for PD was most effective by using the sensor affixed to the affected limb.

To allow for validation of the results, the analysis presented in this paper focused only on the recorded data segments corresponding to specific in-clinic tests. The methodologies can, however, be extended to analysis of data over the entire duration of the recordings, providing useful information on the temporal prevalence of specific motor symptoms in specific individuals and in characterizing individual variations to medication and other interventions. Such analysis is key to providing personalized and responsive treatment regimens for PD and HD, which is an objective of our ongoing research.

5. REFERENCES

[1] Parkinson's Disease Foundation, "What is Parkinson's

This paper appears as K. Dinesh, M. Xiong, J. Adams, R. Dorsey, and G. Sharma, "Signal analysis for detecting motor symptoms in parkinson's and huntington's disease using multiple body-affixed sensors: A pilot study," in Proc. IEEE Western NY Image and Signal Proc. Workshop (WNYISPW) , Nov. 2016.

disease?" accessed Oct. 2016. [Online]. Available: http://www.pdf.org/en/about_pd

[2] J. B. Martin and J. F. Gusella, "Huntington's disease," *N. Engl. J. Med*, vol. 315, no. 20, pp. 1267–1276, 1986.

[3] Parkinson's Disease Foundation, "Statistics on Parkinson's," accessed Oct. 2016. [Online]. Available: http://www.pdf.org/en/parkinson_statistics

[4] Huntington Study Group, "How many people have Huntington disease?" accessed Oct. 2016. [Online]. Available: http://huntingtonstudygroup.org/hd-insights/how-many-people-have-huntington-disease/

[5] C. G. etal., "Movement disorder society-sponsored revision of the unified parkinson's disease rating scale (MDS-UPDRS): Scale presentation and clinimetric testing results," *Movement Disorders*, vol. 23, no. 15, pp. 2129–2170, 2008. [Online]. Available: http://dx.doi.org/10.1002/mds.22340

[6] "Unified Huntington's disease rating scale: Reliability and consistency," *Movement Disorders*, vol. 11, no. 2, pp. 136–142, 1996. [Online]. Available: http://dx.doi.org/10.1002/mds.870110204

[7] M. Hassanalieragh, A. Page, T. Soyata, G. Sharma, M. Aktas, G. Mateos, B. Kantarci, and S. Andreescu, "Health monitoring and management using Internet-of-Things (IoT) sensing with cloud-based processing: Opportunities and challenges," in *Proc. of the 12th IEEE Intl. Conf. on Services Computing (SCC 2015)*, New York, NY, USA, Jun. 2015, pp. 285–292.

[8] E. E. Tripoliti, A. T. Tzallas, M. G. Tsipouras, G. Rigas, P. Bougia, M. Leontiou, S. Konitsiotis, M. Chondrogiorgi, S. Tsouli, and D. I. Fotiadis, "Automatic detection of freezing of gait events in patients with Parkinson's disease," *Comp. Methods and Prog. in Biomedicine*, vol. 110, no. 1, pp. 12 – 26, 2013. [Online]. Available: http://www.sciencedirect.com/science/article/pii/S0169260712002787

[9] A. Bermeo, M. Bravo, M. Huerta, and A. Soto, "A system to monitor tremors in patients with Parkinson's disease," in *2016 38th Annual Intl. Conf. of the IEEE Engg. in Med. and Biology Soc. (EMBC)*, Aug 2016, pp. 5007–5010.

[10] B. M. Eskofier, S. I. Lee, J. F. Daneault, F. N. Golabchi, G. Ferreira-Carvalho, G. Vergara-Diaz, S. Sapienza, G. Costante, J. Klucken, T. Kautz, and P. Bonato, "Recent machine learning advancements in sensor-based mobility analysis: Deep learning for Parkinson's disease assessment," in *38th Annual Intl. Conf. of the IEEE Engg. in Med. and Biology Soc. (EMBC)*, Aug 2016, pp. 655–658.

[11] K. L. Andrzejewski *et al.*, "Wearable sensors in huntington disease: a pilot study," *Jour. of Huntington's Disease*, 2016.

[12] "Biostamprc User Manual." [Online]. Available: https://www.mc10inc.com/our-products/biostamprc

[13] T. Heida, E. C. Wentink, and E. Marani, "Power spectral density analysis of physiological, rest and action tremor in parkinsons disease patients treated with deep brain stimulation," *Jour. of Neuroengineering and Rehabilitation*, vol. 10, no. 1, p. 1, 2013.

[14] A. Nadeau, K. Dinesh, M. Xiong, and G. Sharma, "In-situ calibration of accelerometers in body worn sensors using quiescent gravity," submitted to IEEE Intl. Conf. on Acoustics, Speech and Signal Proc. (ICASSP) 2017.

[15] I. Jolliffe, *Principal component analysis*. Wiley Online Library, 2002.

[16] A. V. Oppenheim and R. W. Schafer, *Discrete-time signal processing*. Pearson Higher Education, 2010.